Journal of Organometallic Chemistry, 330 (1987) 279–289
Elsevier Sequoia S.A., Lausanne – Printed in The Netherlands

FORMATION OF A σ-CYCLOBUTYL–PLATINUM BOND BY THE INTRAMOLECULAR ACTIVATION OF A CYCLOBUTYLPHOSPHINE. SYNTHESIS AND STRUCTURE OF $[\overline{Pt(P(t\text{-}Bu)_2CH_2\overline{CHCH_2CH_2C}H)}]_2(\mu\text{-}Br)_2$ *

BARBARA L. SIMMS and JAMES A. IBERS
Department of Chemistry, Northwestern University, Evanston, IL 60201 (U.S.A.)

(Received September 16th, 1986)

Summary

When the hydrobromide adduct of di-t-butylcyclobutylmethylphosphine, $P(t\text{-}Bu)_2(CH_2\overline{CHCH_2CH_2C}H_2) \cdot HBr$ is combined with $K[PtCl_3(C_2H_4)]$ and LiBr in ethanol and heated at reflux for 5 h, the σ-cyclobutyl complex $[\overline{Pt(P(t\text{-}Bu)_2CH_2\overline{CHCH_2CH_2C}H)}]_2(\mu\text{-}Br_2)$ forms. The complex also forms from $[PtBr(P(t\text{-}Bu)_2CH_2\overline{CHCH_2CH_2C}H_2)]_2(\mu\text{-}Br)_2$ in boiling ethanol. The structure of $[\overline{Pt(P(t\text{-}Bu)_2CH_2\overline{CHCH_2CH_2C}H)}]_2(\mu\text{-}Br)_2$ was deduced from spectroscopic and analytical data and confirmed by X-ray analysis of a single crystal. The complex crystallizes in the tetragonal system in space group C_{4v}^{12}-$I4_1cd$ ($a = b = 19.658(7)$ Å, $c = 15.805(6)$ Å, $T = 113$ K) with 8 molecules per unit cell. The final agreement index for $R(F^2)$ is 0.075 for the 2403 unique data (including $F_0^2 < 0$). Bond lengths in the five-membered chelate ring $\overline{Pt\text{–}P\text{–}C(3)\text{–}C(10)\text{–}C}(11)$ are Pt–P 2.198(4), P–C(3) 1.875(18). C(3)–C(10) 1.53(2), C(10–C(11) 1.57(2), C(11)–Pt 2.079(17) Å. The remaining cyclobutyl bond distances are C(11)–C(12) 1.56(2), C(12)–C(13) 1.51(3), C(10)–C(13) 1.53(3) Å. The Pt–Br bond distances are 2.510(2) and 2.612(2) Å for bromine *cis*- and *trans*- to atom C(11), respectively.

Introduction

The interaction of transition-metal complexes with cyclopropanes and cyclobutanes continues to be an important area of interest in organometallic and organic chemistry because of the special reactivity of these alicyclic compounds to C–H and C–C bond activation [1]. The reaction of cyclopropanes with metal complexes to give metallacyclobutanes is a familiar example of bond cleavage by metal insertion

* Prof. L. Sacconi has contributed seminally to the coordination chemistry of multi-dentate ligands and the factors involved in such coordination. It is a pleasure for J.A.I. to dedicate this article to Luigi, a superb scientist, host, and gentleman.

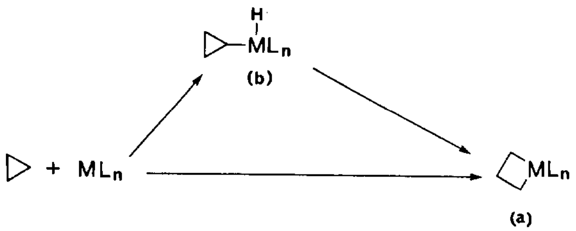

SCHEME 1

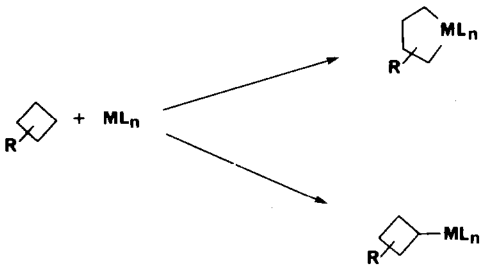

SCHEME 2

into a C–C bond [1c, e; 2] (Scheme 1a). The insertion usually occurs with no observed σ-cyclopropyl intermediate. However, one report of the intramolecular formation of a metallacyclobutane from an initially formed σ-cyclopropyl hydride complex (Scheme 1b) has appeared [1e]. Cyclobutanes are much less reactive than cyclopropanes, but also may be activated by transition-metal complexes (Scheme 2). Insertion of the metal center into a cyclobutane C–C bond gives metallacyclopentanes [2a, c; 3]. Most examples of metallacyclopentanes formed by C–C bond insertion involve extremely strained compounds, such as cubane, that contain multiple fused rings. Both metallacyclopentanes and σ-cyclobutyl complexes have been proposed as intermediates in the isomerization of cyclobutanes to olefins [4] or as intermediates in ring-expansion reactions [5].

Our recent interest in the reactions described above has focused on orthometallation products obtained by reacting bulky cyclopropyl and cyclobutyl phosphines with transition metals [6]. Though a chelating σ-allyl complex, $PtCl(P(t\text{-}Bu)_2CH{=}CMeCH_2)(P(t\text{-}Bu)_2CH_2CHCH_2CH_2)$, forms from *trans*-$PtCl_2(P(t\text{-}Bu)_2CH_2CHCH_2CH_2)_2$ in boiling 2-methoxyethanol [6b], no orthometallation products form from *trans*-$PtCl_2(P(t\text{-}Bu)_2CH_2CHCH_2CH_2CH_2)_2$ [6e]. We proposed that this lack of reactivity occurs owing to the steric environment of cyclobutane in *trans*-$PtCl_2(P(t\text{-}Bu)_2CH_2CHCH_2CH_2CH_2)_2$ and that a subtle change in this environment could result in orthometallation (and cyclobutane activation). Here we report the activation of a cyclobutane C–H bond in $P(t\text{-}Bu)_2(CH_2CHCH_2CH_2CH_2)$ by Pt^{II} to give the dimeric σ-cyclobutyl complex $[Pt(P(t\text{-}Bu)_2CH_2CHCH_2CH_2CH)]_2(\mu\text{-}Br)_2$.

Results and discussion

When equimolar quantities of $K[PtCl_3(C_2H_4)]$ and $P(t\text{-}Bu)_2(CH_2CHCH_2CH_2CH)_2 \cdot HBr$ and three equivalents of LiBr are combined in ethanol and heated at reflux for several hours, the initially orange reaction mixture with some decomposition gradually lightens to give a pale yellow solution. A similar color change without decomposition occurs when $[PtBr(P(t\text{-}Bu)_2CH_2CHCH_2CH_2CH_2)]_2(\mu\text{-}Br)_2$ is heated in boiling ethanol for 5 min. Filtration and cooling of both reaction mixtures results in fine, pale yellow crystals of identical composition. The distinctive loss of color from reactants to products is typical of orthometallation reactions [6a–d]. Chemical analysis of the crystals for C, H, Br, and P are consistent with the empirical formula $C_{13}H_{26}BrPPt$. We concluded that the material is dimeric from the molecular weight of 976 amu, obtained from mass spectral data. There are no olefin absorptions in the IR spectrum. The ^{31}P NMR spectrum from a recrystallized sample contains four singlets near 94.0 ppm. The two largest peaks occur at 94.59 and 94.00 ppm with Pt–P coupling constants 5365 and 5356 Hz, respectively. For comparison the ^{31}P chemical shifts observed for $[PtBr(P(t\text{-}Bu)_2CH_2CHCH_2CH_2CH_2)]_2(\mu\text{-}Br)_2$ is 39.64 ppm ($J_{(P-Pt)}$ = 3864 Hz). The downfield shift of the phosphine resonance upon orthometallation is expected for phosphorus contained in a five-atom metallacycle [7]. Since activation of a t-Bu group would result in a four-membered ring, the observed resonances must arise from products of cyclobutane activation. The increase in the Pt–P coupling constants for the metallated vs. non-metallated phosphine reflects the compression of the Pt–P bond that occurs with ring formation [6c]. Such M–L bond shortening is general in orthometallation reactions [6a,c].

The complex proton spectrum provides little structural information about the products (other than confirming the absence of olefinic protons) since it is dominated by overlapping t-Bu resonances. The ^{13}C NMR spectrum is similarly complex. However, it contains valuable structural information from the phosphorus coupling and chemical shift differences for each type of carbon nucleus in the chelate ring. From the DEPT [8] pulse sequence the resonances not arising from the t-Bu carbon nuclei were assigned as follows: 38 + 48 ppm, CH (two distinct types); 28 + 30 + 33 ppm, CH_2 (three distinct types). These regions of the spectrum are too complex for any Pt–C coupling to be observed. These data are consistent with the structure $[Pt(P(t\text{-}Bu)_2CH_2CHCH_2CH_2CH)]_2(\mu\text{-}Br)_2$ for the isomeric products and argue against alternative structures for the metallacycle such as $Pt(CH_2CH_2CH_2(CH_2)CH_2P(t\text{-}Bu)_2)$ (a [2.2.1]-platinacyclohexane) or PtPCH=CMeCHMe (a σ-allyl platinacyclopentane). Thus C–H and not C–C bond activation of cyclobutane occurs. The observed resonances may arise from *syn-* and *anti*-$[Pt(P(t\text{-}Bu)_2CH_2CHCH_2CH_2CH)]_2(\mu\text{-}Br)_2$ (which interconvert in solution) or from a mixture of diastereomers of one of these geometric forms or both.

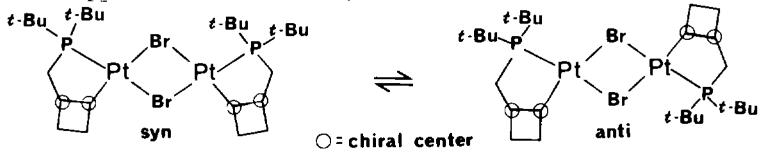

In order to characterize better this unusual [3.2.0]-metallabicycloheptane ring system, we have performed a single-crystal X-ray analysis of the complex. As illustrated in Fig. 1, the molecular structure is that proposed from spectroscopic data, namely $[Pt(P(t\text{-}Bu)_2CH_2CHCH_2CH_2CH)]_2(\mu\text{-}Br)_2$. A single diastereomer of the *anti* configuration crystallizes as a racemic mixture. Each dimeric unit has a crystallographically imposed twofold axis. In these dimers the Pt atoms have a

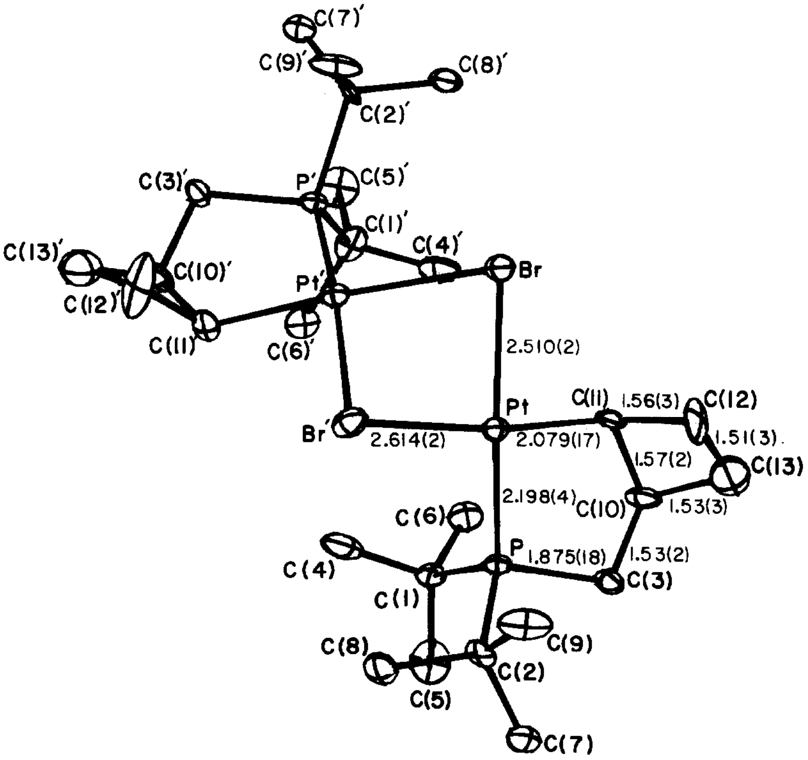

Fig. 1. Structure and numbering scheme for $\overline{PtP(t\text{-}Bu)_2CH_2CHCH_2CH_2CH}]_2(\mu\text{-}Br)_2$. The thermal ellipsoids are drawn at the 50% probability level. The figure shows important bond distances for the structure.

distorted *cis*-square planar geometry; each belongs to a five-membered chelate ring in addition to being bonded to two bridging bromine atoms. The shortest intermolecular non-hydrogen separation (3.47(3) Å) occurs between methyl carbon atoms C(5) and C(8) of neighboring molecules. Bond distances involving the Pt coordination sphere and the metallacycle are shown in Fig. 1 while Table 1 lists intramolecular bond distances and angles between non-hydrogen atoms.

The chelate ring is formally part of a [3.2.0]-metallabicycloheptane in which the metallacycle shares atoms C(10) and C(11) with a cyclobutyl ring comprised of atoms C(10)–C(13). The PtPC(10)C(11) portion of the ring is planar (average deviation 0.015 Å). The distances from this plane to the remaining chelate ring atoms are C(3), 0.47, C(12) 1.38, and C(13) 1.07 Å. Thus the platinacyclopentane ring adopts an envelope conformation with near-normal tetrahedral angles for C and P atoms. The C(10)–C(13) cyclobutyl ring is in a butterfly conformation very similar to that adopted by cyclobutane in *trans*-$PtCl_2(P(t\text{-}Bu)_2CH_2\overline{CHCH_2CH_2CH_2})_2$ [6e]. The deviations from the best least-squares plane for the C_4 ring are C(10), −0.07(2), C(11), 0.06(2), C(12), −0.19(3), and C(13) 0.10(2) Å. The angle between this plane and the PtPC(10)C(11) plane is 51.5°.

Bond distances and angles in the C_4 ring are similar to those observed for cyclobutane in *trans*-$PtCl_2(P(t\text{-}Bu)_2CH_2\overline{CHCH_2CH_2CH_2})_2$ [6e]. The Pt–C(11)

TABLE 1

BOND DISTANCES (Å) AND ANGLES (°) IN $[\overline{Pt(P(t\text{-}Bu)_2CH_2CHCH_2CH_2CH)}]_2(\mu\text{-}Br)_2$

Pt···Pt′ [a]	3.234(1)	C(1)–C(5)	1.55(2)
Pt–Br	2.510(2)	C(1)–C(6)	1.58(3)
Pt–Br′	2.614(2)	C(2)–C(7)	1.54(2)
Pt–P	2.198(4)	C(2)–C(8)	1.57(2)
Pt–C(11)	2.079(17)	C(2)–C(9)	1.54(2)
Br···Br′	3.423(4)	C(3)–C(10)	1.53(2)
P–C(1)	1.84(2)	C(10)–C(11)	1.57(2)
P–C(2)	1.88(2)	C(10)–C(13)	1.53(3)
P–C(3)	1.88(2)	C(11)–C(12)	1.56(3)
C(1)–C(4)	1.53(2)	C(12)–C(13)	1.51(3)
Br–Pt–Br′	83.79(7)	C(4)–C(1)–C(6)	106.1(14)
Br–Pt–P	172.3(1)	C(5)–C(1)–C(6)	107.3(14)
Br′–Pt–P	102.2(1)	P–C(2)–C(7)	113.1(12)
Br–Pt–C(11)	89.1(4)	P–C(2)–C(8)	111.9(12)
Br′–Pt–C(11)	172.3(4)	P–C(2)–C(9)	107.0(11)
P–Pt–C(11)	85.3(4)	C(7)–C(2)–C(8)	110.2(13)
Pt–Br–Pt′	78.22(5)	C(7)–C(2)–C(9)	108.2(16)
Pt–P–C(1)	111.0(5)	C(8)–C(2)–C(9)	106.1(15)
Pt–P–C(2)	117.0(5)	P–C(3)–C(10)	108.4(12)
Pt–P–C(3)	105.4(5)	C(3)–C(10)–C(11)	112.9(14)
C(1)–P–C(2)	112.8(8)	C(3)–C(10)–C(13)	113.2(17)
C(1)–P–C(3)	105.8(8)	C(11)–C(10)–C(13)	86.2(15)
C(2)–P–C(3)	103.6(7)	Pt–C(11)–C(10)	118.5(10)
P–C(1)–C(4)	110.8(13)	Pt–C(11)–C(12)	115.2(14)
P–C(1)–C(5)	113.9(12)	C(10)–C(11)–C(12)	88.5(15)
P–C(1)–C(6)	108.0(11)	C(11)–C(12)–C(13)	87.0(15)
C(4)–C(1)–C(5)	110.4(15)	C(10)–C(13)–C(12)	92.3(16)

[a] Primed atoms are related to the corresponding unprimed atoms by the crystallographic twofold axis.

bond length, 2.079(17) Å, is close to the Pt–C bond length in $[\overline{Pt(P(t\text{-}Bu)_2CH_2CMe_2CH_2)}]_2(\mu\text{-}Cl)_2$, 2.06 Å [12], but is slightly longer than the Pt–C bond length of 2.018(6) Å in $\overline{PtCl(P(t\text{-}Bu)_2CH{=}C(CH_3)CH_2})(\overline{P(t\text{-}Bu)_2CH_2CHCH_2CH_2})$ [6b].

Distortions from exact planar geometry for ligands about the Pt atom result from the envelope conformation adopted by the metallacycle. Thus while the Pt, P, and C(11) atoms along with the Br atom lie essentially in the best least-squares plane calculated for the PtBrBr′CP unit, the Br′ atom is 0.18(1) Å above this plane. The dihedral angle between the two $PtBr_2CP$ units is 70.0°. The Pt–Br bond distances of 2.510(2) and 2.614(2) Å for Br atoms *cis* and *trans* to atom C(11), respectively, are normal for Pt–Br bonds that occur *trans* to highly *trans*-directing ligands such as phosphines and alkyls. The bond distances differ because of the more substantial *trans* influence of the alkyl ligand. The Pt–Br bond distance for the Br atom *trans* to atom C(11) (2.614(2)) is longer than the Pt–Br bonds in *trans*-$PtBr(\eta^1\text{-allyl})(PEt_3)_2$ (2.543(1) Å) [9] and in *trans*-$PtBr(\eta^1\text{-styryl})(PPh_3)_2$ (2.502(1) Å) [10] but close to the 2.629(7) Å Pt–Br bond length reported for $[PtMe_3]_2(\mu\text{-}Br)_2(\mu\text{-}Se_2Me_2)$, in which the bridging Br atoms are *trans* to the methyl C atoms [11]. The Pt–P bond distance, 2.198(4) Å, is the same as that in the structurally similar chelate complex $[\overline{Pt(P(t\text{-}Bu)_2CH_2CMe_2CH_2)}]_2(\mu\text{-}Cl)_2$, 2.200 Å [12], but is significantly shorter than the Pt–P bond in $[Pt(PEt_3)(SnCl_3)]_2(\mu\text{-}Cl)_2$, 2.230(2) Å [13]. The shorter Pt–P bond lengths in the orthometallated complexes are expected [6a,c].

The cyclometallation of $[PtBr(P(t\text{-}Bu)_2CH_2CHCH_2CH_2CH_2)](\mu\text{-}Br)_2$ proceeds easily relative to that of either *trans*-$PtCl_2(P(t\text{-}Bu)_2CH_2CHCH_2CH_2)$ [6b] or *trans*-$PtCl_2(P(t\text{-}Bu)_2CH_2CHCH_2CH_2CH_2)_2$ (which does not undergo any cyclometallation) [6e]. Several factors may be responsible for the observed reactivity pattern. Electronic factors include differences in electronegativity and polarizability of Br vs. Cl. Steric factors include greater congestion in the non-metallated bromo-bridged dimer or a more favorable approach route between Pt and cyclobutane in this dimer (vs. the *trans*-$PtCl_2P_2$ monomer). The results obtained here enable us to put forth a steric argument. For monomeric *trans*-PtX_2P_2 complexes, orthometallation reactions occur most easily when X = I or Br and less easily for X = Cl, NO_3, or OAc [14]. However, dimeric complexes $Pt_2X_4P_2$ are less sterically congested and usually undergo orthometallation reactions more slowly than comparable *trans*-PtX_2P_2 monomers [6c,15]. This generalization may not apply, however, if the bulky phosphine ligand contains alkyl groups with very different steric requirements. Thus *trans*-$PtCl_2(P(t\text{-}Bu)_2CH_2CH_2CHCH_2CH_2)_2$ is unreactive to orthometallation but $[PtX(P(t\text{-}Bu)_2CH_2CH_2CHCH_2CH_2)]_2(\mu\text{-}X)_2$ (X = Cl, Br) readily loses halide with cyclopropyl ring opening to give *cis*-$PtX_2(P(t\text{-}Bu)_2CH_2CH_2CH{=}CHCH_3)$ [6d].

If the preferred torsion angles in the non-metallated complex are very similar to those in the metallated complex, the energy barrier to orthometallation is lowered [16]. However, if preferred torsion angles must be greatly compressed for the reactive C–C or C–H bond to approach the metal center, orthometallation may not occur. As shown in Fig. 2, the alkyl groups on each phosphine ligand in *trans*-$PtCl_2(P(t\text{-}Bu)_2CH_2CHCH_2CH_2CH_2)_2$ adopt a staggered conformation around the P–Pt–P bond axis. For a C–H (or C–C) bond of cyclobutane to approach the Pt atom, the methyl cyclobutyl alkyl group must bend towards the C(5)′ t-Bu group,

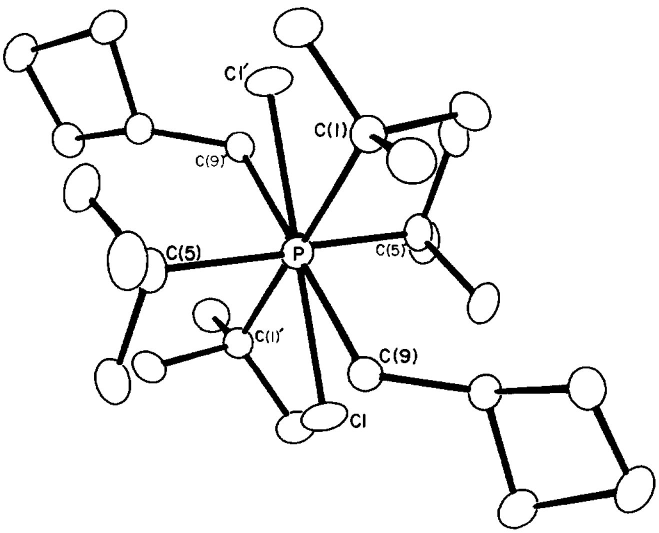

Fig. 2. A view down the P–Pt–P bond axis showing the staggering of ligands in *trans*-$PtCl_2(P(t\text{-}Bu)_2CH_2CHCH_2CH_2CH_2)_2$.

perhaps requiring some rotation of the Pt–P bond and thus *gauche* interactions between the methyl groups of atoms C(5) and C(1)′ and those of atom C(1) with atom Cl′. The presence of these steric constraints in the monomer may prevent orthometallation despite the steric relief orthometallation would impart. This steric relief is most strikingly illustrated by the contrasting P–CH_2–(cyclobutane) bond angles in $PtCl_2(P(t\text{-}Bu)_2CH_2CHCH_2CH_2CH_2)_2$ (118.1(2)°) [6e] and in [Pt(P(t-Bu)$CH_2CHCH_2CH_2CH)]_2(\mu\text{-}Br)_2$ (108.4(12)°). Thus steric forces in *trans*-$PtCl_2(P(t\text{-}Bu)_2CH_2CHCH_2CH_2CH_2)_2$ that are subtly different from those in $[PtBr(P(t\text{-}Bu)_2CH_2CHCH_2CH_2CH_2)]_2(\mu\text{-}Br)_2$ may hinder the approach of cyclobutane to the Pt atom. In the same way one may explain the preference for C–H over C–C bond activation in the cyclometallation of the $Pt_2Br_4P_2$ dimer. Changes in the preferred torsion angles may be least pronounced for approach of the C–H bond to the Pt center.

Experimental section

General remarks

All reactions were carried out under prepurified dinitrogen with the use of standard Schlenk-line techniques. Di-t-butyl(cyclobutylmethyl)phosphonium hydrobromide was prepared as described previously [6e]. $K[PtCl_3(C_2H_4)]$ was used as received from Aldrich Chemical Company. Solvents were purified by standard methods.

Elemental analyses were performed by Micro-Tech Laboratories, Skokie, IL. Infrared spectra were obtained with a Perkin–Elmer 283 spectrometer from samples prepared as KBr pellets. ^1H, ^{13}C, and ^{31}P NMR spectra were recorded on a JEOL FX90Q, a JNM-FX270, or a Varian FX400 FT-NMR spectrometer. Mass spectral data were collected with a Hewlett Packard 5985 spectrometer.

Synthesis of $[Pt(P(t\text{-}Bu)_2CH_2CHCH_2CH_2CH)]_2(\mu\text{-}Br)_2$

A mixture of $K[PtCl_3(C_2H_4)]$ (0.50 g, 0.0014 mol), $P(t\text{-}Bu)_2(CH_2CHCH_2CH_2CH_2)\cdot HBr$ [6e] (0.40 g, 0.0014 mol), and LiBr (0.35 g, 0.004 mol) were heated at reflux for 5 h in anhydrous EtOH. During this period the color of the reaction mixture changed from orange to pale yellow. The reaction mixture was filtered to remove Pt metal (from decomposition), LiX, and KX (X = Cl, Br). EtOH was distilled from the filtrate under vacuum. The pale orange residue was crystallized from $CHCl_3$, isolated yield 41% (0.425 g). The IR spectrum displayed no olefinic stretching frequencies. ^1H NMR ($CDCl_3$) complex cyclobutyl and t-butyl regions. ^{31}P NMR ($CDCl_3$) δ 94.59 (J(P–Pt) 5365 Hz), 94.00 (J(P–Pt) 5356 Hz), 93.78 (J(P–Pt) 5343.6 Hz), 93.58 (J(P–Pt) 5383.2 Hz). ^{13}C NMR δ 43.38 + 43.09 + 42.88 (s, CH), 39.10 + 38.84 (s, CH), 35.52 (br m, CMe_3), 33.00 (d, CH_2, J(P–C) 31.8 Hz) 30.26 (d, CH_2, J(P–C) 17.1 Hz), 29.30 + 29.12 + 29.08 + 28.93 (s, CCH_3), 28.05 (d, CH_2, J(P–C) 14.7 Hz). Anal. Found: C, 31.98; H, 5.29; P, 6.07; Br, 16.02 (no detectable Cl). $C_{26}H_{52}Br_2P_2Pt_2$ calc.: C, 31.96; H, 5.33, P, 6.35; Br, 16.39%.

Alternative synthesis of $[Pt(P(t\text{-}Bu)_2CH_2CHCH_2CH_2CH)]_2(\mu\text{-}Br)_2$. *Synthesis of* $[PtBr(P(t\text{-}Bu)_2CH_2CHCH_2CH_2CH_2)]_2(\mu\text{-}Br)_2$

$K[PtCl_3(C_2H_4)]$ (0.80 g, 0.0022 mol) and $P(t\text{-}Bu)_2(CH_2CHCH_2CH_2CH_2)\cdot HBr$ (0.64 g, 0.0022 mol) were stirred together in anhydrous ethanol for 15 min at 25°C.

The solvent was removed under vacuum. The orange product (^{31}P NMR ($CDCl_3$) δ 36.48 (J(P–Pt) 3964.6 Hz), 44.56 (J(P–Pt) 3940.8 Hz)) was stirred with excess LiBr in boiling acetone for 5 h. Filtration of LiX from the reaction mixture followed by evaporation (under vacuum) of acetone from the filtrate gave red-orange [PtBr(P(t-Bu)$_2$CH$_2$CHCH$_2$CH$_2$CH$_2$)]$_2$(μ-Br)$_2$ in 66% overall yield (0.82 g). ^1H NMR ($CDCl_3$) δ 2.89 (br, 2H) 2.30 (d, J 6.2 Hz, 2H), 1.90 (br, 1H), 1.73 (m, 4H), 1.42 (d, J(P–H) 13.9 Hz, 18 H). ^{31}P NMR ($CDCl_3$) δ 39.64 (s, J(P–Pt) 3863.8 Hz). ^{13}C NMR

TABLE 2

CRYSTAL AND REFINEMENT DATA FOR [Pt(P(t-Bu)$_2$CH$_2$CHCH$_2$CH$_2$CH)]$_2$(μ-Br)$_2$

Molecular formula	$C_{26}H_{52}Br_2P_2Pt_2$
Formula wt. (amu)	976.64
Space group	C_{4v}^{12}-$I4_1cd$
a (Å)	19.658(7) [a]
b (Å)	19.658
c (Å)	15.805(6)
V (Å^3)	6107.7
Z	8
T of data collection	113 K [b]
Crystal vol. (mm^3)	0.00177
ρ, calc. (g/cm^3)	2.125
Radiation	graphite monochromated Mo-K_α ($\lambda(K\alpha_1) = 0.7093$ Å)
Linear absorption coefficient (cm^{-1})	119.6
Transmission factors	0.365–0.457 [c]
Take-off angle (°)	2.00
Scan mode	ω
Scan speed (° min^{-1})	2.00
Scan range (°)	−0.45 to +0.45 in ω
Background counts	extension of 1/4 scan range on each side
Rescan condition	$I \leq 3\sigma(I)$ rescanned for a maximum of 60 s
Data collected [d]	$h, k, \pm l$ ($4.0 \leq 2\theta \leq 36.0$); h, k, l ($2\theta > 36.0$)
2θ limits (°)	$4.0 \leq 2\theta \leq 58.0$
Unique data [e]	2403
Unique data ($F_0^2 > 3\sigma(F_0^2)$)	1487
p factor	0.05
Final no. variables	144
$R(F^2)$ (incl. $F_0^2 < 0$)	0.075
$R_w(F^2)$ (incl. $F_0^2 < 0$)	0.114
$R(F)$ for $F^2 > 3\sigma(F_0^2)$	0.043
Error in observation of unit weight	0.86

[a] Cell parameters were refined under the constraints $a = b$ and $\alpha = \beta = \gamma = 90°$. [b] The low-temperature system for the Nonius CAD 4 diffractometer is based on a design by Prof. J.J. Bonnet and S. Askenazy and is commercially available from Soterem, Z.T. de Vic, 31320 Castanet-Tolosan, France. [c] The analytical method as employed in the Northwestern absorption program AGNOST was used for the absorption correction (J. de Meulenaer and H. Tompa, Acta Crystallogr., 19 (1965) 1014). [d] Subject to the condition $h + k + l = 2n$. [e] Friedel pairs (i.e., hkl and khl) were not both included.

(CDCl$_3$) δ 36.84 (d, J(P–C) = 25.7 Hz, CMe$_3$), 32.86 (d, J(P–C) = 5.5 Hz, CH), 32.26 (d, J(P–C) = 5.5 Hz, 2 cyclobutylmethylene), 30.44 (s, CCH$_3$), 18.17 (s, CHCH$_2$$CH_2CH_2$). Anal. Found: C, 27.51; H, 4.70; P, 5.32; Br, 27.88. $C_{26}H_{54}Br_4P_2Pt_2$ calc.: C, 27.42, H, 4.74; P, 5.44; Br, 28.08%. Heating [PtBr(P(t-Bu)$_2$CH$_2$CHCH$_2$CH$_2$CH$_2$)]$_2$(μ-Br)$_2$ in boiling EtOH for 5 min gave [Pt(P(t-Bu)$_2$CH$_2$CHCH$_2$CH$_2$CH)]$_2$(μ-Br)$_2$ in > 90% yield.

X-Ray study of [Pt(P(t-Bu)$_2$CH$_2$CHCH$_2$CH$_2$CH)]$_2$(μ-Br)$_2$

Crystals suitable for X-ray diffraction study were obtained as parallelepipeds by slow evaporation of a CHCl$_3$ solution of [Pt(P(t-Bu)$_2$CH$_2$CHCH$_2$CH$_2$CH)]$_2$(μ-Br)$_2$. Lattice constants were obtained from least-squares analysis of 25 reflections that had been centered on a Nonius CAD4 diffractometer. Systematic absences in the data hkl: $h+k+l=2n$; $0kl$; k, $l=2n$; hhl; $2h+l=4n$) together with the presence of tetragonal symmetry are strongly indicative of the non-centrosymmetric space group C_{4v}^{12}-$I4_1cd$. Six standard reflections monitored every 3 h during data collection showed no significant decomposition. Friedel pairs (h, k, $\pm l$) were collected in the range $4° \leq 2\theta \leq 36°$ to be used for determination of the direction of the polar axis in the chosen crystal. Details of data collection and refinement are summarized in Table 2. Procedures and programs used are those standard for this laboratory [17].

The position of the Pt atom was determined from a Patterson map. The positions of the remaining non-hydrogen atoms were obtained from a series of electron density syntheses performed with data from which reflections having $l < 0$ had been eliminated.

Least-squares refinement of two isotropic models was next performed. Model A proceeded from the original solution; in model B the signs of the indices were changed. In each model anomalous scattering for Pt, Br, and P was included. The R

TABLE 3

POSITIONAL PARAMETERS AND EQUIVALENT ISOTROPIC THERMAL PARAMETERS FOR [Pt(P(t-Bu)$_2$CH$_2$CHCH$_2$CH$_2$CH)]$_2$(μ-Br)$_2$

Atom	x	y	z	B (Å^2)
Pt	0.021552(28)	0.079376(28)	0	1.24(1)
Br	0.085014(89)	−0.018755(86)	−0.06405(12)	1.93(4)
P	−0.02467(20)	0.16385(19)	0.07065(26)	1.24(8)
C(1)	−0.05434(90)	0.13540(87)	0.1753(12)	2.0(4)
C(2)	−0.08934(72)	0.21683(85)	0.0133(12)	1.8(4)
C(3)	0.04654(82)	0.22505(88)	0.0915(11)	1.6(4)
C(4)	−0.10308(98)	0.0752(11)	0.1668(14)	2.8(5)
C(5)	−0.0871(11)	0.1924(11)	0.22912(94)	2.7(5)
C(6)	0.00931(97)	0.10806(87)	0.2261(11)	2.1(4)
C(7)	−0.09440(88)	0.28976(91)	0.0474(13)	2.1(4)
C(8)	−0.16132(89)	0.18243(95)	0.0131(13)	2.2(4)
C(9)	−0.0669(11)	0.2204(11)	−0.0797(11)	2.5(5)
C(10)	0.11295(86)	0.18469(93)	0.0977(13)	2.2(4)
C(11)	0.11387(82)	0.12036(86)	0.0390(12)	1.8(4)
C(12)	0.1521(12)	0.1637(12)	−0.0292(15)	4.0(6)
C(13)	0.1692(12)	0.2127(12)	0.0410(16)	3.3(6)

indices for models A and B were 0.057 and 0.045, respectively. Of more significance, examination of the 133 Friedel pairs $(hkl, hk\bar{l})$ in which $|F_0(hkl)|$ differs from $|F_0(hk\bar{l})|$ by more than 5% indicates that model B provides the correct sense of the difference for 122 sets. Clearly model B correctly defines the direction of the polar axis in the chosen crystal and it was adopted for ensuing calculations.

After the atoms were refined anisotropically, approximate positional parameters for the methyl hydrogen atoms were obtained from difference electron density maps. These parameters along with the positional parameters for methylene and methyne hydrogen atoms were then idealized. In these calculations a C–H bond length of 0.95 Å was assumed and a given H atom was assigned an isotropic thermal parameter 1 $Å^2$ greater than the equivalent isotropic thermal parameter of the carbon atom to which it is attached. Parameters for the hydrogen atoms were held fixed during the final least-squares cycle on F^2. Table 3 presents the final positional parameters for non-hydrogen atoms with equivalent isotropic thermal parameters. Tables 4 and 5 list the hydrogen atom positions and the anisotropic thermal parameters [18]. Table 6 contains a listing of $10|F_0|$ vs. $10|F_c|$ [18].

Acknowledgment

We are grateful to the National Science Foundation (Grant CHE83-08076) for financial support.

References

1 (a) M. Parra-Hake, M.F. Rettig, J.L. Williams, and R.M. Wing, Organometallics, 5 (1986) 1032; (b) F.J. Liotta, Jr. and B.K. Carpenter, J. Am. Chem. Soc., 107 (1985) 6426; (c) P.W. Jennings, R.E. Ekeland, M.D. Waddington, and T.W. Hanks, J. Organomet. Chem., 285 (1985) 429; (d) T.C. Flood and J.A. Statler, Organometallics, 3 (1984) 1795; (e) R.A. Periana and R.G. Bergman, J. Am. Chem. Soc., 106 (1984) 7272.
2 (a) S. Sarel, Acc. Chem. Res., 11 (1978) 204; (b) J. Rajaram and J.A. Ibers, J. Am. Chem. Soc., 100 (1978) 829; (c) K.C. Bishop, Chem. Rev., 76 (1976) 461; (d) K.G. Powell and F.J. McQuillin, Tetrahedron Lett., (1971) 3313.
3 R. Ros, M. Lenarda, N.B. Pahor, M. Calligaris, P. Delise, L. Randaccio, and M. Graziani, J. Chem. Soc., Dalton Trans., (1976) 1937.
4 (a) R. Houriet, L.F. Halle, and J.L. Beauchamp, Organometallics, 2 (1983) 1818; (b) A. Stockis and R. Hoffmann, J. Am. Chem. Soc., 102 (180) 2952; (c) I.J. Harvie and F.J. McQuillin, Chem. Commun., (1974) 806.
5 N. Chatani, H. Furukawa, T. Kato, S. Murai, and N. Sonoda, J. Am. Chem. Soc., 106 (1984) 430.
6 (a) W.J. Youngs, J. Mahood, B.L. Simms, P.N. Swepston, J.A. Ibers, M. Shang, J. Huang, and J. Lu, Organometallics, 2 (1983) 917; (b) W.J. Youngs and J.A. Ibers, Organometallics, 2 (1983) 979; (c) B.L. Simms, M. Shang, J. Lu, W.J. Youngs, and J.A. Ibers, Organometallics, in press; (d) B.L. Simms and J.A. Ibers, J. Organomet. Chem., 327 (1987) 125; (e) B.L. Simms and J.A. Ibers, J. Organomet. Chem., 327 (1987) 137.
7 P.E. Garrou, Chem. Rev., 81 (1981) 41.
8 (a) M.R. Bendall, D.M. Doddrell, and D.T. Pegg, J. Am. Chem. Soc., 103 (1981) 4603; (b) D.M. Doddrell, D.T. Pegg, and M.R. Bendall, J. Magn. Reson., 48 (1982) 323.
9 J.C. Huffman, M.P. Laurent, and J.K. Kochi, Inorg. Chem., 16 (1977) 2639.
10 J. Rajaram, R.G. Pearson, and J.A. Ibers, J. Am. Chem. Soc., 96 (1979) 2103.
11 E.W. Abel, A.R. Kahn, K. Kite, K.G. Orrell, V. Šik, T.S. Cameron, and R. Cordes, J. Chem. Soc., Chem. Commun., (1979) 713.
12 R. Mason, M. Textor, N. Al-Salem, and B.L. Shaw, J. Chem. Soc., Chem. Commun., (1976) 292.
13 H.C. Clark, G. Ferguson, A.B. Goel, and B.L. Ruhl, Organometallics, 3 (1984) 15.

14 B.L. Shaw, J. Organomet. Chem., 200 (1980) 307 and references therein.
15 (a) N.W. Alcock and P.G. Leviston, J. Chem. Soc., Dalton Trans., (1974) 1834; (b) R.G. Goel; W.O. Ogini and R.C. Srivastava, Organometallics, 1 (1982) 819.
16 A.R.H. Bottomley, C. Crocker and B.L. Shaw, J. Organomet. Chem., 250 (1983) 617.
17 J.M. Waters and J.A. Ibers, Inorg. Chem., 16 (1977) 3273.
18 Supplementary material includes hydrogen atom positoins (Table 4), anisotropic thermal parameters (ORTEPII-Type 8) (Table 5) and structure amplitudes (Table 6). See NAPS document no. 04482 for 14 pages of supplementary material. Order from NAPS c/o Microfiche Publications, P.O. Box 3513, Grand Central Station, New York, N.Y. 10163. Remit in advance in U.S. funds only $7.75 for photocopies or $4.00 for microfilm. Outside the U.S. and Canada add postage of $4.50 for the first 20 pages and $4.00 for each 10 pages of material thereafter. $1.50 for microfiche postage.